Disentangling reaction mechanisms for α production in the ^{6}Li + ^{209}Bi reaction

S. Santra,[1,*] S. Kailas,[1] V. V. Parkar,[1,†] K. Ramachandran,[1] V. Jha,[1] A. Chatterjee,[1] P. K. Rath,[2] and A. Parihari[2]

[1]*Nuclear Physics Division, Bhabha Atomic Research Centre, Mumbai 400085, India*

[2]*The M. S. University of Baroda, Vadodara – 390002, India*

(Received 26 September 2011; revised manuscript received 20 December 2011; published 30 January 2012)

Inclusive breakup α cross sections ($\sigma_{\alpha}^{\rm incl}$) are measured for the ^{6}Li + ^{209}Bi reaction at bombarding energies $E_{\rm lab}$ = 24–50 MeV. The $\sigma_{\alpha}^{\rm incl}$ was observed to be a substantial fraction of the total reaction cross section over the entire energy range, and it exhausts almost whole of the reaction cross section at sub-barrier energies. An investigation on the origin of large inclusive α reveals that most of the α particles are produced by noncapture breakup (^{6}Li $\rightarrow \alpha + d$) and incomplete fusion via d capture. The combined cross sections of noncapture breakup, d capture, and transfer reactions successfully explain the origin of most of the experimental $\sigma_{\alpha}^{\rm incl}$ over the measured energy range. A comparison of the $\sigma_{\alpha}^{\rm incl}$ versus reduced energies for several targets involving ^{6}Li as projectile shows that the cross sections are independent of target. Interestingly, the difference between reaction and complete fusion cross sections "$\sigma_{\rm reac} - \sigma_{\rm CF}$" for several reactions also shows the same behavior.

DOI: 10.1103/PhysRevC.85.014612 PACS number(s): 25.70.Bc, 25.70.Hi, 25.70.Jj

I. INTRODUCTION

The observation of a large cross section for inclusive α produced by breakup and different transfer channels for reactions involving weakly bound projectiles with cluster structure '$\alpha + x$' is well established [1–9]. It has been observed that the production of α in a reaction is much higher compared to that of the valence cluster x. It is a very challenging task to understand the reaction mechanisms responsible for such a large cross section of inclusive α. Attempts have been made to understand the origin of such a large α cross section but it is far from fully understood. Kelly *et al.*, in a study for ^{6,7}Li + ^{208}Pb reaction [1], have shown that the cross sections for exclusive breakup of ^{6}Li(^{7}Li) into $\alpha + d(t)$ are much lower than the measured inclusive α. They suggested that α produced from transfer channels could be very important. Castaneda *et al.* [10] in their detailed work on ^{6}Li + ^{197}Au reaction have found that these α's can be produced by direct as well as sequential processes. They have observed that almost 50% of the inclusive α can be explained in terms of ^{6}Li $\rightarrow \alpha + d$ and ^{6}Li $\rightarrow$ ^{5}Li $\rightarrow \alpha + p$ exclusive breakup channels. The origin of the remaining cross sections were not clear. Assuming the cross section for $1p$ stripping followed by breakup "^{6}Li $\rightarrow$ ^{5}He $\rightarrow \alpha + n$" to be same as $1n$ stripping followed by breakup "^{6}Li $\rightarrow$ ^{5}Li $\rightarrow \alpha + p$" they have somehow explained the origins of most of the inclusive α. However, this assumption is not true. From the coupled reaction channels calculations it can be found that the cross section for $1p$ stripping is much smaller than that for $1n$ stripping, and hence leaving an open question on the description of the origin of the α production. In a similar study for ^{6}Li + ^{208}Pb system, Signorini *et al.* [4] have found that the combined cross sections of exclusive breakup of ^{6}Li into $\alpha + d$ and $1n$-stripping followed by breakup (^{6}Li $\rightarrow$ ^{5}Li $\rightarrow \alpha + p$) also cannot explain the large cross section for inclusive α. They suggested many other possible channels that might contribute to the rest of the α particles. Partial fusion or stripping breakup is known to be one of the important channels that produces a large number of α particles in several reactions [11–14]. In one of the studies for ^{7}Li + ^{159}Tb reaction [14] Utsunomiya *et al.* have found that roughly a half of the α and triton yield is originated from the breakup-fusion process, in which one of the breakup fragments is captured by a target nucleus. So, it would be highly interesting to estimate the α contribution from all possible channels including the breakup-fusion and understand the origin of the measured inclusive α for the present system ^{6}Li + ^{209}Bi.

Another interesting observation is that the systematics made by different authors [5–7] for the reactions involving ^{6}Li show that the inclusive breakup-α cross section follow a universal curve with respect to the normalized energy ($E_{\rm c.m.}/V_b$). It is surprising because both breakup and transfer reactions, which are supposed to be the main contributors, are peripheral reactions whose cross sections are expected to increase with the size of the target nuclei. Besides, the transfer contributions that depend on the target structure could be quite different. So, it would be interesting to revisit this issue involving a different target (^{209}Bi), and understand the production mechanism by disentangling the contributions of breakup and transfer channels.

This paper is organized as follows. The details of the measurements of inclusive α cross sections are given in Sec. II. The data analysis, the results of the coupled-channels calculations, incomplete/breakup fusion calculations by "sum-rule" method, and the origin of large α production are discussed in Sec. III. Systematics of inclusive α cross sections is discussed in Sec. IV. Finally, the results are summarized in Sec. V.

II. MEASUREMENTS

The inclusive breakup α cross sections were measured for ^{6}Li + ^{209}Bi reaction at energies $E_{\rm lab}$ = 24–50 MeV using

*ssantra@barc.gov.in

†Present address: Departamento de Física Aplicada, Universidad de Huelva, E-21071 Huelva, Spain.

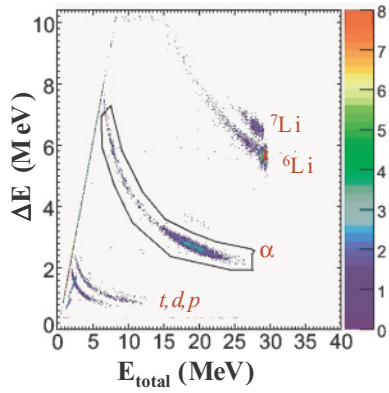

FIG. 1. (Color online) A typical two dimensional spectrum of ΔE versus E_{total} for $^{6}\text{Li} + ^{209}\text{Bi}$ measured by a telescope at $\theta_{\text{lab}} = 118^{\circ}$ and $E_{\text{beam}} = 32$ MeV.

^{6}Li beam from the BARC-TIFR 14-UD pelletron facility in Mumbai. The self-supporting target (^{209}Bi), with a thickness of $\sim$330 μg/cm^2 was prepared by vacuum evaporation technique. Four ΔE-E telescopes of Si surface barrier detectors were placed 10° apart on a movable arm inside a 1 m diameter scattering chamber to detect the projectile like fragments. Each telescope with 5 mm diameter collimator has an angular spread of $\pm 0.5^{\circ}$. The telescopes, with detector thickness of $\Delta E = 25$–33 μm and $E = 500$–1000 μm, were suitable for detection of particles with $Z = 1$, 2, and 3. Two monitors of single surface barrier detectors of thickness 2000 μm were placed at $\pm 25^{\circ}$ of either side of the beam for cross section normalization as well as beam monitoring. A typical 2D spectrum measured by a telescope at $\theta_{\text{lab}} = 118^{\circ}$ for $E_{\text{beam}} = 32$ MeV is shown in Fig. 1.

III. ANALYSIS AND DISCUSSION

A. Inclusive breakup α

Figure 2 shows typical 1D projections of α-spectra measured at the grazing angles for several incident beam energies. It can be observed that a broad ($\sim$8–10 MeV) but distinct α peak, with centroid equal to two-thirds of the projectile energy, is possibly due to the projectile breakup ($^{6}\text{Li} \rightarrow \alpha + d$) by either direct or sequential processes. A statistical model calculation shows that the spectrum of α evaporation from complete fusion is far lower in energy. Assuming the breakup proceeding dominantly with low excitation ($\epsilon \leqslant 1$ MeV) as observed in Ref. [15], the energy width "$E_{\text{max}} - E_{\text{min}}$" of the α peaks are expected (from Eq. (1) of Ref. [4]) to be $\sim$8–10 MeV for the entire energy and angular range. Using these energy limits of the α particles, the angular distributions of the inclusive breakup α are extracted and shown in Fig. 3(a) and 3(b). The maximum of these distributions are found to occur at grazing angles. Some nonsmooth behavior in the angular distributions for low beam energies (24–30 MeV) is due to (i) uneven background subtractions in four different telescopes and (ii) low statistics. Similar background was also observed for $^{6,7}\text{Li} + ^{208}\text{Pb}$ [1].

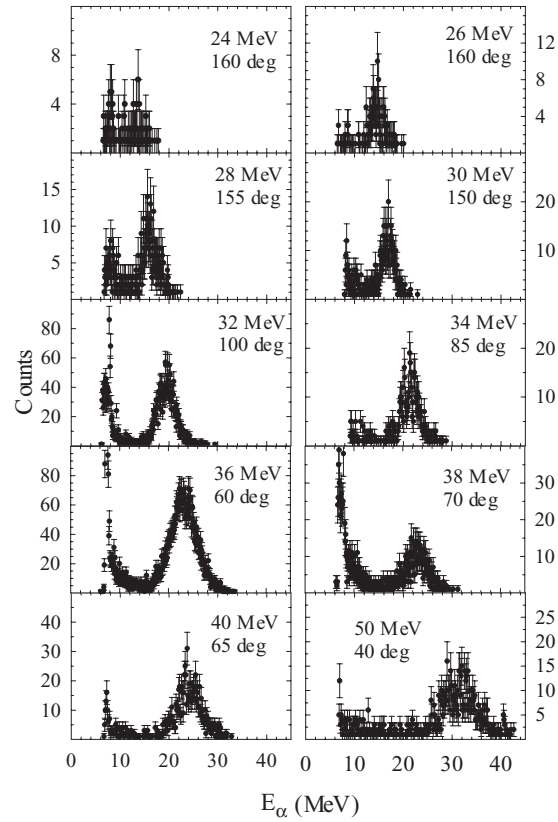

FIG. 2. Inclusive α spectra at $\theta \sim \theta_{gr}$ for different bombarding energies.

The above background in α spectrum could arise due to the target impurities like ^{12}C and ^{16}O. Figure 2 illustrates the positions of the low energy α background with respect to the high energy α peak of our interest. It can be observed that the main (high-energy) peak is well separated from the background. In a typical α spectrum detected at $\theta_{\text{lab}} = 100^{\circ}$ for 32 MeV ^{6}Li beam (see Fig. 2), let us calculate the energy positions of the breakup α's produced from the interaction with ^{12}C, ^{16}O, and ^{209}Bi targets. Assuming the breakup of ^{6}Li into α and d proceeding dominantly through the 3^{+} resonant state of ^{6}Li, one can calculate the reaction kinematics. The expected breakup α peaks corresponding to ^{12}C and ^{16}O targets are in the range of $\sim$5–8 MeV, however it is $\sim$19 MeV for ^{209}Bi target which are found to be consistent with the measurement. Since the broadening of the main peak is $\sim$9 MeV, the α particles arising from C and O contaminations could be well separated. So, in the inclusive breakup α data, there is no contribution of α coming from the O and C impurities. It can be observed from Fig. 2 that the separation of the α particles produced by the target and background gradually increases with the increase of the incident beam energy. For a particular beam energy, the separation also increases at backward angles. However, at lower energies and forward angles, the separation decreases which leads to an increase in the uncertainty in the extraction of α yield and hence the inclusive data.

The measured angular distribution data (with proper background subtraction) were first fitted with arbitrary functions by χ^2 minimization as shown by lines in Fig. 3. The fitted

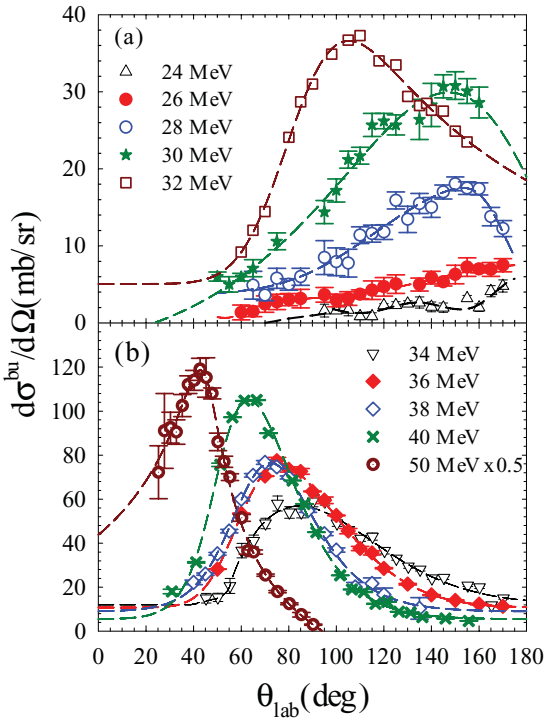

FIG. 3. (Color online) Inclusive breakup α angular distribution for ^{6}Li + ^{209}Bi at energies (a) $E_{\rm lab}$ = 24–32 MeV and (b) $E_{\rm lab}$ = 34–50 MeV. Lines are χ^2 minimized fit to the data and used to obtain the angle integrated cross sections.

curves were used to obtain the angle integrated cross sections. In Fig. 4(a), the angle integrated cross sections of inclusive breakup-α (hollow triangles-up) are compared with the cross sections for total reaction $\sigma_{\rm reac}$ (dotted line) obtained from OM fit to the elastic scattering by Santra *et al.* [16], experimental complete fusion (CF, stars) and complete+incomplete fusion (CF+ICF, hollow triangles-down) data [17]. It shows that inclusive breakup is the major reaction channel at energies near and below the Coulomb barrier. It was interesting to find that the sum of $\sigma_{\rm CF}$ and $\sigma_{\alpha}^{\rm incl}$ (hollow squares) exhaust all of $\sigma_{\rm reac}$ predicted by OM over the entire energy range of our interest.

To investigate the energy dependence behavior of different reactions, the probabilities of all the significant channels with respect to total reaction cross sections at different energies are compared in Fig. 4(b). The dominant reaction channels were found to be inclusive breakup-α (filled triangles), CF (filled stars), and ICF (filled circles). At sub-barrier energies, it was interesting to find that while going down in energy, the contribution of $\sigma_{\alpha}^{\rm incl}$ to $\sigma_{\rm reac}$ increases and its behavior is just opposite to that of CF and inelastic (dash-dot line) cross sections. The noncapture breakup cross section (dashed line) behavior calculated by the continuum discretized coupled-channels (CDCC) method is also found to be similar to $\sigma_{\alpha}^{\rm incl}$. This again confirms that when all the other channels start closing at sub-barrier energies, the breakup channel does not close which is consistent with the observation of nonzero imaginary potential at these energies [16].

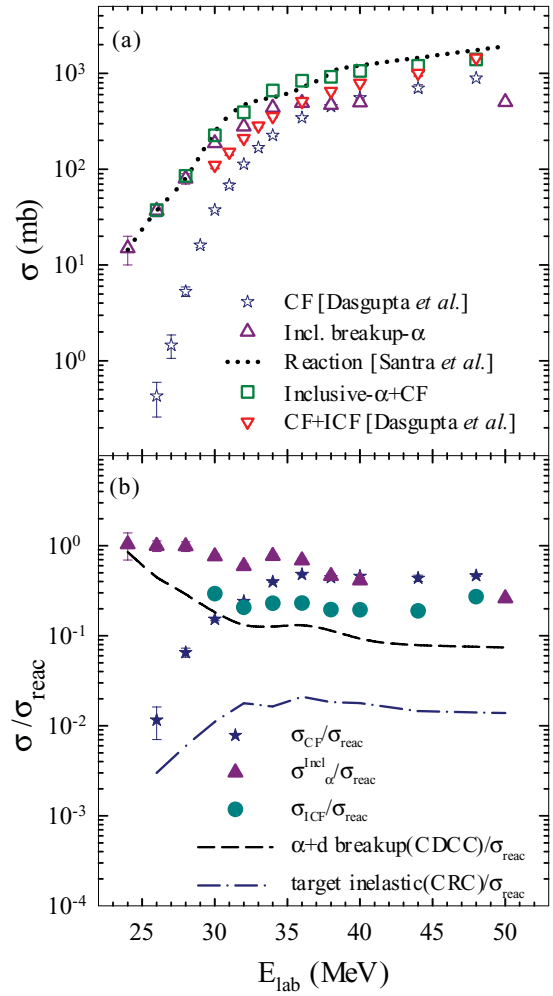

FIG. 4. (Color online) (a) Comparison of the angle integrated inclusive breakup-α cross sections (present data) with the cross sections for total reaction $\sigma_{\rm reac}$ obtained from OM fit [16], complete fusion [17], and complete+incomplete fusion [17]. (b) Normalized cross sections for inclusive α ($\sigma_{\alpha}^{\rm incl}$), CF ($\sigma_{\rm CF}$), ICF ($\sigma_{\rm ICF}$), noncapture $\alpha + d$ breakup, and target inelastic channels with respect to total reaction cross section ($\sigma_{\rm reac}$), showing their relative contributions.

B. Coupled-channels calculations

To understand the reaction mechanism involved in the above observations coupled-channels calculations were made using FRESCO [18]. For CDCC calculations, the ^{6}Li was taken as a cluster of $\alpha + d$ for its bound as well as continuum (resonant and nonresonant) states. The breakup of the projectile into its fragments (α and d) is considered to be caused by inelastic excitations to different partial waves ($l = 0, 1, 2$) in the continuum (up to an excitation energy of 8.0 MeV), induced by the projectile fragments-target interactions due to Coulomb as well as nuclear forces. For s and p waves, the continuum was discretized into 16 bins of equal width in the momentum of $\alpha - d$ relative motion. In the presence of resonances for d waves, the discretization of the continuum was slightly modified in order to avoid double counting. The resonance regions are discretized into larger number of bins, i.e., with smaller momentum steps. The couplings of the

ground state to the continuum, continuum to continuum, and reorientation coupling are included. The CDCC calculations were performed using the cluster-folded interaction [19], where α-target ($V_{\alpha+\mathrm{Bi}}$) and deuteron-target ($V_{d+\mathrm{Bi}}$) optical potentials are evaluated at $E_\alpha \approx \frac{2}{3}E_{6\mathrm{Li}}$ and $E_d \approx \frac{1}{3}E_{6\mathrm{Li}}$, respectively. The $V_{\alpha+\mathrm{Bi}}$ potential used in our calculations was taken from Ref. [20] for $E_{\mathrm{lab}} = 24.8$ MeV. Both the real and the imaginary potentials were of Woods-Saxon volume form and the parameters are $v_0 = 107.4$ MeV, $r_0 = 1.361$ fm, $a_0 = 0.578$ fm, $w = 13.5$ MeV, $r_w = 1.412$ fm, $a_w = 0.299$ fm. Similarly, the $V_{d+\mathrm{Bi}}$ potential, with real parameters $v_0 = 100.2$ MeV, $r_0 = 1.15$ fm, $a_0 = 0.973$ fm, and imaginary parameters $w = 15.37$ MeV, $r_w = 1.45$ fm, $a_w = 0.559$ fm, were taken to be same as that of $d + {}^{208}$Pb at 12 MeV [21]. Imaginary parts of $V_{\alpha+\mathrm{Bi}}$ and $V_{d+\mathrm{Bi}}$ describe the removal of flux whenever the individual fragments themselves breakup, excite, or fuse with the target. The strengths of the real part of $V_{\alpha+\mathrm{Bi}}$ as well as $V_{d+\mathrm{Bi}}$ have been adjusted by a scale factor of 0.8 to 1.0 compared to the values in Refs. [20,21] in order to explain the elastic data in the measured energy range of 24–50 MeV [16].

To calculate the cross sections for inelastic and transfer channels coupled reaction channels (CRC) calculations are performed. The CDCC derived effective potentials ($\Delta V_p + V_{\mathrm{bare}}$ and $\Delta W_p + W_{\mathrm{bare}}$ that include the effect of projectile breakup) are used for the entrance channel. We have coupled (i) 17 inelastic states corresponding to the multiplets of ^{208}Pb(3^- and 5^-)$\bigotimes \pi h_{9/2}$, and (ii) transfer couplings that include only low-lying excited states of the outgoing transfer partitions with six channels for $1n$ pickup (${}^7\mathrm{Li} + {}^{208}\mathrm{Bi}$), two channels each for $1n$ stripping (${}^5\mathrm{Li} + {}^{210}\mathrm{Bi}$) and $1p$ stripping (${}^5\mathrm{He} + {}^{210}\mathrm{Po}$) reactions. All the nonelastic channels are coupled to the entrance channel only. The inelastic states were treated as collective vibrational states and their form factors were chosen to be the derivatives of the potentials. The β values [22] and the deformation lengths are same as those used in Ref. [23]. Reduced deformation lengths (Coulomb and nuclear) were calculated and used for each possible transition corresponding to the same collective vibrational states. For transfer partitions, the real potentials were calculated using the semiemperical parametrization of folding model potentials given by Broglia and Winther [24]:

$$U_n(r) = -31.67\frac{R(A_1)R(A_2)}{R(A_1)+R(A_2)} \times \left[1+\exp\left(\frac{r-R(A_1,A_2)}{a}\right)\right]^{-1} \mathrm{MeV}, \quad (1)$$

where, $R(A) = 1.233A^{\frac{1}{3}} - 0.98A^{-\frac{1}{3}}$ fm and $R(A_1, A_2) = R(A_1) + R(A_2) + \Delta R$ fm with the diffuseness parameter set to $a = 0.63$ fm and the free parameter $\Delta R = 0.2$ fm. The imaginary potential for the transfer channels were of Woods-Saxon squared form with a depth of 50 MeV, a radius parameter of 1.0 fm and a diffuseness parameter of 0.4 fm. The potentials binding the transferred particles were of Woods-Saxon form, with radius $1.2A^{\frac{1}{3}}$ fm and diffuseness 0.6 fm, their depths being automatically adjusted to obtain the required binding energies. Spectroscopic factors are taken from the literature [23,25]. Results are shown in Figs. 4 and 6.

C. Incomplete/breakup fusion

The energetic charged particles (lighter than the projectiles) peaked at forward angles have been observed in a number of heavy ion reactions leading to fusion like products and these processes are interpreted as massive transfer or incomplete fusion [26–34]. The experimental ICF cross section for the present system is already known to be very large [17]. So, the probability of one of the breakup fragments (say d) fusing with ^{209}Bi and the complementary fragment (α) flying out to contribute to $\sigma_\alpha^{\mathrm{incl}}$ is also significant. Since the experimentally observed ICF cross section by Dasgupta *et al.* [17] is equal to the sum of p-capture, d-capture, and α-capture cross sections, one needs to separate the individual cross sections to estimate the noncaptured α contribution from the ICF data. There is no simple method available to estimate the above cross sections for the incoming energies below as well as above the Coulomb barrier. A recently developed three-body classical dynamical model by Diaz-Torres *et al.* [35] can be used to calculate the individual ICF cross sections using a breakup probability function.

The ICF events are known to occur for a narrow range of entrance channel angular momentum ℓ_i starting just above the critical angular momentum ℓ_{cr} [12,33]. Wilczynski [12] have proposed a method known as "sum-rule" using which it was possible to explain the cross sections for different ICF channels in the reaction of ${}^{14}\mathrm{N} + {}^{159}\mathrm{Tb}$ at a bombarding energy of 140 MeV. However, in a theoretical study by Udagawa *et al.* for the ^{181}Ta(^{14}N,α) reaction [13], it has been observed that the ICF is not necessarily a peripheral reaction instead it occurs at deep (∼2 fm inside) peripheral region, also the associated angular momentum is less than l_{cr}. In case of ${}^{19}\mathrm{F} + {}^{89}\mathrm{Y}$,^{66}Zn [36,37], and many other reactions, the experimental ICF cross sections are found to be much higher than the "sum-rule" predictions as energy decreases toward the Coulomb barrier implying that the contribution from $\ell < \ell_{\mathrm{cr}}$ could also be present in the observed ICF. So, a modified "sum rule," that extends the angular momentum window toward lower ℓ values, has been employed to reproduce the ICF cross sections for ${}^{19}\mathrm{F} + {}^{66}\mathrm{Zn}$ [37]. An energy dependent factor was required to reproduce the ICF data. Another problem is that the original sum rule model cannot predict the cross section at sub-barrier energies. But, for the present system the data for both CF and ICF are available at energies below as well as above the Coulomb barrier. In order to calculate these cross sections and reproduce the experimental data (as constraints) we varied two parameters of the original "sum rule" with energy. One of the two important parameters is r_c that fixes the Coulomb barrier, $V_c = r_c(A_p^{1/3} + A_t^{1/3})$, and decides on the total fusion (CF+ICF) cross section. The second parameter q_c calculates the change in Coulomb interaction energy, $Q_c = q_c(Z_1^f Z_2^f - Z_1^i Z_2^i)$, and determines the reaction probabilities for all the reactions. The probability for ith reaction channel proceeding via the partially equilibrated system is proportional to the exponential factor as proposed by Bondorf *et al.* [38]:

$$p(i) \sim e^{[Q_{gg}(i)-Q_c(i)]/T}, \quad (2)$$

where $Q_{gg}(i)$ is the ground state Q value of the ith channel and T is an effective temperature which is kept fixed at 2.5 MeV.

TABLE I. Parameters r_c and q_c used in the "sum rule" calculations for different beam energies.

E_{lab} (MeV)	r_c (fm)	q_c (MeV)
24	1.089	0.001
26	1.178	0.001
28	1.267	0.240
30	1.337	0.520
32	1.400	0.710
34	1.430	0.780
36	1.450	0.810
38	1.480	0.860
40	1.500	0.880
44	1.550	0.880
48	1.550	0.820
50	1.550	0.820

The parameters r_c and q_c used in the "sum-rule" calculations for different beam energies are given in Table I.

The results of the 'sum-rule' calculations are shown in Fig. 5. It can be observed from Fig. 5(a) that d-capture cross sections (dash-dot-dot line) are most dominating followed by proton (dash-dot line) and α capture (dotted line) as expected from the ground state Q-value consideration (Q_{gg} for d, p and α-transfer channels are 5.836 MeV, 0.390 MeV, and -10.73 MeV, respectively). Combined cross sections for p, d, and α captures are represented by a dashed line. Cross sections of some of the above channels normalized to total reaction cross section are given in Fig. 5(b) to see their relative contributions as a function of energy. It can be observed that the behavior of the ICF channels at sub-barrier energies is similar to the noncapture breakup channels implying that all these channels are connected to the breakup mechanism.

D. Disentangling α contributions

To unfold the production mechanisms for such a large cross section for $\sigma_\alpha^{\text{incl}}$, the coupled-channels calculations were performed as described in Sec. III B. The results of the important channels along with the exclusive experimental data are shown in Fig. 6. Reactions that might contribute to the α-production are (i) noncapture breakup of ^{6}Li $\rightarrow \alpha + d$, (ii) $\alpha + d$ breakup followed by d capture (part of ICF), (iii) neutron stripping followed by breakup (^{6}Li $\rightarrow {}^5$Li $\rightarrow \alpha + p$), (iv) proton stripping followed by breakup (^{6}Li $\rightarrow {}^5$He $\rightarrow \alpha + n$), (v) deuteron stripping transfer (^{6}Li,α), and (vi) neutron pickup transfer followed by breakup (^{6}Li $\rightarrow {}^7$Li $\rightarrow \alpha + t$). However, the major contributions to inclusive α production were found to be the first three processes. Present calculations and exclusive measurements reported in Ref. [15] show that contributions from last three processes are negligible. CDCC calculations show that the total (direct + sequential) noncapture "$\alpha + d$" breakup (dashed line) is dominated by the sequential breakup through 3^+ resonance state of ^{6}Li (dot-dashed line). It may be mentioned that the breakup due to Coulomb interaction was dominant over nuclear interaction. But, nuclear breakup was found to play a major role to explain the experimental data specially at backward angles as observed in Ref. [15].

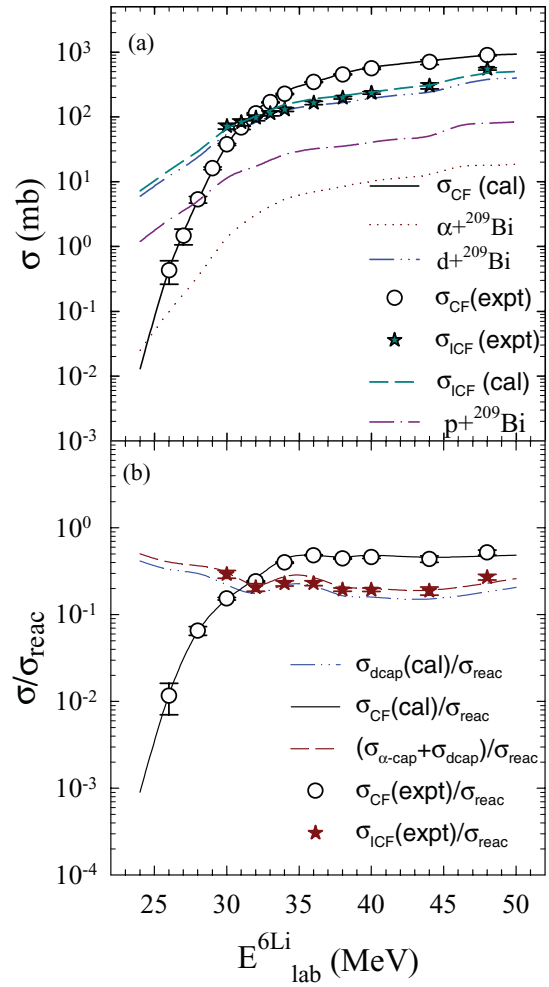

FIG. 5. (Color online) (a) Calculated cross sections by sum-rule model for CF (solid line), d-capture (dash-dot-dot line), p-capture (dash-dot line), and α-capture (dotted line) as a function of beam energy are compared with the experimental CF (hollow circles) and ICF (stars) data [17]. Dashed line represents the calculated total ICF cross sections. (b) Corresponding cross sections normalized to σ_{reac} to show their relative contributions to the total reaction cross section.

The second contribution to α production comes from ICF or breakup fusion. α contribution from the ICF is same as d-capture/transfer cross section which was obtained in Sec. III C employing "sum-rule" method is shown as a dash-dot-dot line in Fig. 6.

Among transfer reactions, (^{6}Li, ^{5}Li)and (^{6}Li, ^{5}He) reactions are very important. Since, ^{5}Li and ^{5}He are unstable they will immediately breakup into α and p/n, and hence the transfer cross sections are equal to their contribution toward α production cross section. However, in the process (vi) all of ^{7}Li produced may not break into $\alpha + t$. In the exclusive breakup measurements done earlier [15] it has been found that the cross section for $\alpha + t$ breakup is negligible. CRC calculations show that the processes (iv) and (v) also contribute very little to the α production. Maximum contribution from the transfer reactions comes from the "^{6}Li $\rightarrow {}^5$Li $\rightarrow \alpha + p$" process (dotted line). But, the calculated cross sections are much less than our previously measured values (stars) at

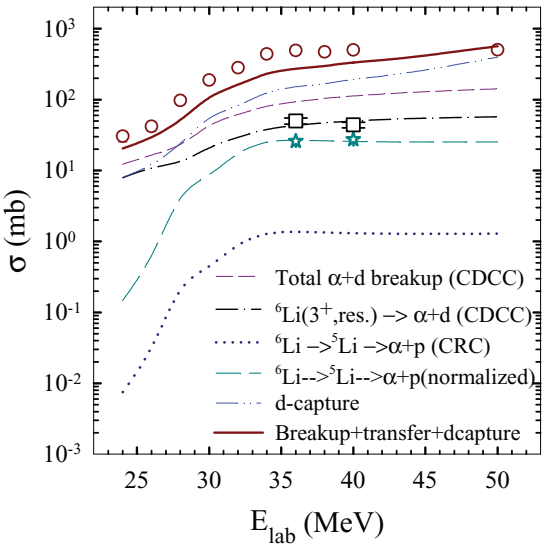

FIG. 6. (Color online) Inclusive breakup α (circles, present data) and α contributions from different transfer and breakup channels (see text for details). Squares and stars represent data on exclusive "$d + \alpha$" (sequential) breakup and "$p + \alpha$" breakup [15], respectively.

$E_{\rm lab} = 36$ and 40 MeV [15]. This may be due to the coupling of only few low lying transfer excited states. For ^{6}Li + ^{208}Pb [10], it was shown that most of the "$\alpha + p$" contributions are via the transfer "$^{6}\mathrm{Li} \rightarrow {}^{5}\mathrm{Li}$" at optimum Q-value (−7.7 MeV). A recent exclusive measurement on ^{6}Li + ^{208}Pb at $E_{\rm lab} =$ 29 MeV [39] shows that the cross section for "$\alpha + p$" breakup is even higher than "$\alpha + d$" breakup specially at higher relative energies. So, the measured cross section for "$\alpha + p$" breakup in the ^{6}Li + ^{209}Bi reaction could be a lower limit as mentioned earlier [15]. However, it is difficult to calculate the absolute cross section corresponding to all the relative energies as the spectroscopy factors are not known for higher excited states of the outgoing $1n$ transfer channel. Thus the cross section values obtained only from the low lying excited states were normalized to the measured data at two energies to estimate the realistic "$\alpha + p$" contribution (long-dashed line).

Combined cross section of total "$\alpha + d$", "$\alpha + p$" (normalized), and d capture, shown by a solid line, was found to be pretty close to the measured $\sigma_{\alpha}^{\rm incl}$ but slightly smaller than the measured values. Difference between the theory and the data could possibly arise due to the lower limit in the contribution from the "$\alpha + p$" channel as mentioned above.

IV. SYSTEMATICS OF INCLUSIVE α

To test the universality of the α production in the reactions involving the weakly bound ^{6}Li projectile and targets with different masses and atomic numbers such as ^{28}Si [6], ^{58}Ni, ^{118,120}Sn [5], ^{59}Co [8], ^{90}Zr [7], ^{208}Pb [2,40], and ^{209}Bi, $\sigma_{\alpha}^{\rm incl}$ was plotted in Fig. 7(a) as a function of normalized energy ($E_{\rm c.m.}/V_b$). The value of V_b for the present system was taken to be 30.1 MeV from Ref. [17] where it has been derived from the precisely measured fusion excitation function and barrier

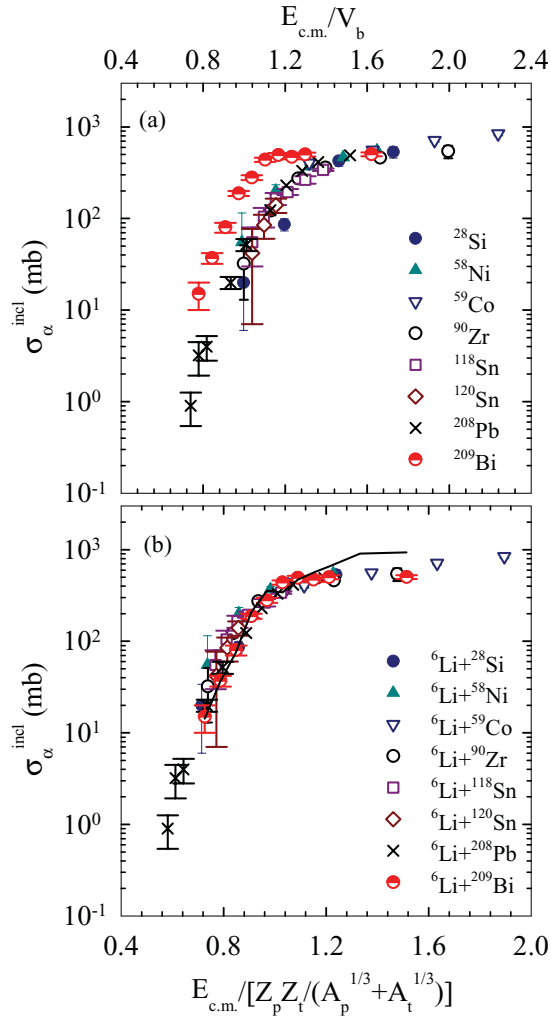

FIG. 7. (Color online) Inclusive breakup α cross sections involving ^{6}Li projectile with several different targets including ^{209}Bi (present data) as a function of (a) $E_{\rm c.m.}/V_b$ and (b) $E_{\rm c.m.}/[Z_pZ_t/(A_p^{1/3} + A_t^{1/3})]$. The solid line in (b) represents the values of "$\sigma_{\rm reac} - \sigma_{\rm CF}$" for ^{6}Li + ^{209}Bi.

distribution. V_b for the rest of the systems are taken to be same as in Refs. [5–7]. It was interesting to see that cross sections for the present system do not fall in the universal curve as described in Refs. [5–7]. The reason was found to be due to the use of inconsistent value of the Coulomb barrier (V_b) which are obtained from two different methods. The one is taken to be equal to the energy at which the backscattering cross section deviates from the Rutherford cross section, and the other is the average fusion barrier from the measured barrier distribution. For some of the above systems for which none of the measurements are available the V_b has been obtained by scaling the Z value of the target with respect to a system whose barrier is measured. It was found that the V_b for ^{6}Li + ^{208}Pb was taken to be 25 MeV [5] which is ∼5 MeV smaller than the nearby and present system ^{6}Li + ^{209}Bi. However, by Z scaling the expected V_b for these two systems should be within ±0.4 MeV. Also, from the comparative study of ^{12}C + ^{208}Pb and ^{12}C + ^{209}Bi reactions [41] it is known that ^{208}Pb and ^{209}Bi

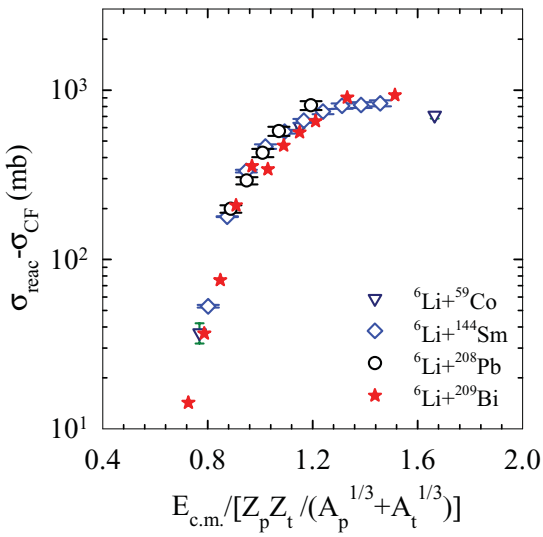

FIG. 8. (Color online) The difference in reaction and complete fusion cross sections ($\sigma_{\rm reac} - \sigma_{\rm CF}$) for several systems involving ^{6}Li as a projectile as a function of $E_{\rm c.m.}/[Z_pZ_t/(A_p^{1/3} + A_t^{1/3})]$.

nuclei behave similarly. Thus the observed difference in α cross sections corresponding to the latter two target nuclei could be just an artifact of inconsistent V_b values.

In order to remove the inconsistency in the values of V_b which are obtained by different methods for different systems, a modified formula for energy normalization was employed. Here the V_b was assumed to be proportional to $Z_pZ_t/(A_p^{1/3} + A_t^{1/3})$, where Z_p (Z_t) and A_p(A_t) are atomic number and atomic masses of the projectile (target), respectively. The $\sigma_\alpha^{\rm incl}$ versus the above normalized energies for different systems are replotted in Fig. 7(b). Interestingly, it can be observed that now the inclusive α cross section for all the above systems follow a universal curve.

Assuming the α production to be the dominant direct reaction mechanism, the difference in the reaction cross section obtained from the OM analysis [16] and the complete fusion cross section [17] i.e., "$\sigma_{\rm reac} - \sigma_{\rm CF}$" was calculated for $^6{\rm Li} + ^{209}{\rm Bi}$ [solid line in Fig. 7(b)] which also shows a similar trend and compares well with $\sigma_\alpha^{\rm incl}$ data specially at low energies where the above assumption is valid. Encouraged by this observation the values of "$\sigma_{\rm reac} - \sigma_{\rm CF}$" are also derived for several other reactions involving ^{6}Li as projectiles, e.g., $^6{\rm Li} + ^{208}{\rm Pb}$, $^6{\rm Li} + ^{144}{\rm Sm}$, and $^6{\rm Li} + ^{59}{\rm Co}$ systems to find the target independence if any. The reaction cross sections for $^6{\rm Li} + ^{59}{\rm Co}$, $^6{\rm Li} + ^{208}{\rm Pb}$, and $^6{\rm Li} + ^{209}{\rm Bi}$ are obtained from Refs. [42], [43], and [16], respectively. For $^6{\rm Li} + ^{144}{\rm Sm}$, the elastic data are available in the literature [44] at several beam energies around the Coulomb barrier. The optical model analyses of the above data were performed using phenomenological potentials and the reaction cross sections were derived for the above energies. The complete fusion cross sections for ^{144}Sm and ^{208}Pb were obtained from the Refs. [45] and [46], respectively. Assuming 30% suppression, the CF for $^6{\rm Li} + ^{59}{\rm Co}$ was obtained from the total fusion measured in Ref. [42]. Finally, the values of "$\sigma_{\rm reac} - \sigma_{\rm CF}$" for these three systems along with the ones for the present system ($^6{\rm Li} + ^{209}{\rm Bi}$) are plotted in Fig. 8 as a function of normalized energy [same as x axis in Fig. 7(b)]. It is interesting to observe that the plots are independent of the targets and the trend is equal to that of $\sigma_\alpha^{\rm incl}$. Thus our assumption that "α production is the major contribution to the reaction cross section other than CF in the reactions involving ^{6}Li" is found to be reasonable. Secondly, the universal behavior of "$\sigma_{\rm reac} - \sigma_{\rm CF}$" for several reactions implies that the direct reaction cross section in the above reactions is independent of the target nuclei. Although $\sigma_{\rm CF}$ and $\sigma_{\rm reac}$ individually did not show a similar behavior.

V. SUMMARY AND CONCLUSIONS

Inclusive breakup α cross sections for $^6{\rm Li} + ^{209}{\rm Bi}$ reaction have been measured at several energies around the Coulomb barrier. The cross section for the above channel was found to be a significant fraction of the total reaction at all the energies, and at sub-barrier energies it exhausts almost whole of the reaction cross section. The comparison of the probabilities of different reaction channels confirms the dominance of breakup channels at sub-barrier energies and it allows the imaginary part of the optical potential to remain nonzero as observed in our earlier study [16].

An investigation on the origin of the large $\sigma_\alpha^{\rm incl}$ shows that the dominant contribution is from d-capture reaction. Most importantly, the combined cross sections of noncapture $\alpha + d$ breakup, d-capture, and transfer reactions could successfully explain the origin of most of the experimental $\sigma_\alpha^{\rm incl}$ over the measured energy range.

A systematics of inclusive α cross section for several reactions involving ^{6}Li as projectile with different targets reveals that they fall on a universal curve as a function of normalized energy. Surprisingly, the difference in reaction and complete fusion cross sections for several reactions involving ^{6}Li as projectile also shows the same trend as that of $\sigma_\alpha^{\rm incl}$, though individually the $\sigma_{\rm reac}$ and $\sigma_{\rm CF}$ do not show any universality.

[1] G. R. Kelly, N. J. Davis, R. P. Ward, B. R. Fulton, G. Tungate, N. Keeley, K. Rusek, E. E. Bartosz, P. D. Cathers, D. D. Caussyn *et al.*, Phys. Rev. C **63**, 024601 (2000).

[2] C. Signorini, M. Mazzocco, G. Prete, F. Soramel, L. Stroe, A. Andrighetto, I. Thompson, A. Vitturi, A. Brondi, M. Cinausero *et al.*, Eur. Phys. J. A **10**, 249 (2001).

[3] R. J. Woolliscroft, N. M. Clarke, B. R. Fulton, R. L. Cowin, M. Dasgupta, D. J. Hinde, C. R. Morton, and A. C. Berriman, Phys. Rev. C **68**, 014611 (2003).

[4] C. Signorini, A. Edifizi, M. Mazzocco, M. Lunardon, D. Fabris, A. Vitturi, P. Scope, F. Soramel, L. Stroe, G. Prete *et al.*, Phys. Rev. C **67**, 044607 (2003).

[5] K. O. Pfeiffer, E. Speth, and K. Bethge, Nucl. Phys. A **206**, 545 (1973).

[6] A. Pakou, N. Alamanos, A. Gillibert, M. Kokkoris, S. Kossionides, A. Lagoyannis, N. G. Nicolis, C. Papachristodoulou, D. Patiris, D. Pierroutsakou, Phys. Rev. Lett. **90**, 202701 (2003).

[7] H. Kumawat, V. Jha, V. V. Parkar, B. J. Roy, S. Santra, V. Kumar, D. Dutta, P. Shukla, L. M. Pant, A. K. Mohanty *et al.*, Phys. Rev. C **81**, 054601 (2010).

[8] F. Souza, C. Beck, N. Carlin, N. Keeley, R. L. Neto, M. de Moura, M. Munhoz, M. D. Santo, A. Suaide, E. Szanto *et al.*, Nucl. Phys. A **821**, 36 (2009).

[9] A. Shrivastava, A. Navin, N. Keeley, K. Mahata, K. Ramachandran, V. Nanal, V. Parkar, A. Chatterjee, and S. Kailas, Phys. Lett. B **633**, 463 (2006).

[10] C. M. Castaneda, H. A. Smith Jr., P. P. Singh, and H. Karwowski, Phys. Rev. C **21**, 179 (1980).

[11] J. H. Barker, J. R. Beene, M. L. Halbert, D. C. Hensley, M. Jaaskelainen, D. G. Sarantites, and R. Woodward, Phys. Rev. Lett. **45**, 424 (1980).

[12] J. Wilczynski, K. Siwek-Wilczynska, J. van Driel, S. Gonggrijp, D. C. J. M. Hageman, R. V. F. Janssens, J. Lukasiak, and R. H. Siemssen, Phys. Rev. Lett. **45**, 606 (1980).

[13] T. Udagawa, D. Price, and T. Tamura, Phys. Lett. B **118**, 45 (1982).

[14] H. Utsunomiya, S. Kubono, M. H. Tanaka, M. Sugitani, K. Morita, T. Nomura, and Y. Hamajima, Phys. Rev. C **28**, 1975 (1983).

[15] S. Santra, V. Parkar, K. Ramachandran, U. Pal, A. Shrivastava, B. Roy, B. Nayak, A. Chatterjee, R. Choudhury, and S. Kailas, Phys. Lett. B **677**, 139 (2009).

[16] S. Santra, S. Kailas, K. Ramachandran, V. V. Parkar, V. Jha, B. J. Roy, and P. Shukla, Phys. Rev. C **83**, 034616 (2011).

[17] M. Dasgupta, P. R. S. Gomes, D. J. Hinde, S. B. Moraes, R. M. Anjos, A. C. Berriman, R. D. Butt, N. Carlin, J. Lubian, C. R. Morton *et al.*, Phys. Rev. C **70**, 024606 (2004).

[18] I. Thompson, Comput. Phys. Rep. **7**, 167 (1988).

[19] F. G. Perey and G. Satchler, Nucl. Phys. A **97**, 515 (1967).

[20] P. Singh, A. Chatterjee, S. K. Gupta, and S. S. Kerekatte, Phys. Rev. C **43**, 1867 (1991).

[21] P. Christensen, A. Berinde, I. Neamu, and N. Scintei, Nucl. Phys. A **129**, 337 (1969).

[22] T. P. Cleary, N. Stein, and P. R. Maurenzig, Nucl. Phys. A **232**, 287 (1974).

[23] S. Santra, P. Singh, S. Kailas, A. Chatterjee, A. Navin, A. Shrivastava, A. M. Samant, and K. Mahata, Phys. Rev. C **60**, 034611 (1999).

[24] R. A. Broglia and A. Winther, *Heavy Ion Reactions*, Parts I and II (Addison-Wesley, Redwood City, CA, 1991).

[25] P. L. Kerr, K. W. Kemper, P. V. Green, K. Mohajeri, E. G. Myers, and B. G. Schmidt, Phys. Rev. C **55**, 2441 (1997).

[26] S. L. Tabor, L. C. Dennis, and K. Abdo, Phys. Rev. C **24**, 2552 (1981).

[27] S. L. Tabor, L. C. Dennis, K. W. Kemper, J. D. Fox, K. Abdo, G. Neuschaefer, D. G. Kovar, and H. Ernst, Phys. Rev. C **24**, 960 (1981).

[28] M. Sasagase, M. Sato, S. Hanashima, K. Furuno, Y. Nagashima, Y. Tagishi, S. M. Lee, and T. Mikumo, Phys. Rev. C **27**, 2630 (1983).

[29] S. J. Padalino and L. C. Dennis, Phys. Rev. C **31**, 1794 (1985).

[30] S. L. Tabor, L. C. Dennis, and K. Abdo, Nucl. Phys. A **391**, 458 (1982).

[31] T. Inamura, M. Ishihara, T. Fukuda, T. Shimoda, and H. Hiruta, Phys. Lett. B **68**, 51 (1977).

[32] D. R. Zolnowski, H. Yamada, S. E. Cala, A. C. Kahler, and T. T. Sugihara, Phys. Rev. Lett. **41**, 92 (1978).

[33] K. Siwek-Wilczynska, E. H. du Marchie van Voorthuysen, J. van Popta, R. H. Siemssen, and J. Wilczynski, Phys. Rev. Lett. **42**, 1599 (1979).

[34] K. A. Geoffroy, D. G. Sarantites, M. L. Halbert, D. C. Hensley, R. A. Dayras, and J. H. Barker, Phys. Rev. Lett. **43**, 1303 (1979).

[35] A. Diaz-Torres, Comput. Phys. Commun. **182**, 1100 (2011).

[36] R. Tripathi, K. Sudarshan, S. Sodaye, and A. Goswami, J. Phys. (London) G **35**, 025101 (2008).

[37] R. Tripathi, K. Sudarshan, S. Sodaye, A. V. R. Reddy, A. Goswami, B. K. Nayak, and S. K. Sharma, Phys. Rev. C **79**, 064604 (2009).

[38] J. P. Bondorf, F. Dickmann, D. H. E. Gross, and P. J. Siemens, J. Phys. (Paris), Colloq. **32**, C6 (1971).

[39] D. Luong, M. Dasgupta, D. Hinde, R. du Rietz, R. Rafiei, C. Lin, M. Evers, and A. Diaz-Torres, Phys. Lett. B **695**, 105 (2011).

[40] R. Ost, E. Speth, K. O. Pfeiffer, and K. Bethge, Phys. Rev. C **5**, 1835 (1972).

[41] S. Santra, P. Singh, S. Kailas, A. Chatterjee, A. Shrivastava, and K. Mahata, Phys. Rev. C **64**, 024602 (2001).

[42] C. Beck, N. Keeley, and A. Diaz-Torres, Phys. Rev. C **75**, 054605 (2007).

[43] N. Keeley, S. Bennett, N. Clarke, B. Fulton, G. Tungate, P. Drumm, M. Nagarajan, and J. Lilley, Nucl. Phys. A **571**, 326 (1994).

[44] J. M. Figueira, J. Niello, A. Arazi, O. A. Capurro, P. Carnelli, L. Fimiani, G. V. Marti, D. Heimann, A. E. Negri, A. J. Pacheco, Phys. Rev. C **81**, 024613 (2010).

[45] P. K. Rath, S. Santra, N. L. Singh, R. Tripathi, V. V. Parkar, B. K. Nayak, K. Mahata, R. Palit, S. Kumar, S. Mukherjee *et al.*, Phys. Rev. C **79**, 051601(R) (2009).

[46] Y. W. Wu, Z. H. Liu, C. J. Lin, H. Q. Zhang, M. Ruan, F. Yang,, Z. C. Li, M. Trotta, and K. Hagino, Phys. Rev. C **68**, 044605 (2003).